

uously that the helices of the four subunits had to be arranged in an antiparallel manner. Thus, from considerations of symmetry we could readily ascertain that the basic topology consisted of a four-helix bundle and a pair of antiparallel β sheets. Initial calculations were therefore carried out on the basis of the following NOEs: unambiguous intrasubunit NOEs relating to the secondary structure; intersubunits relating to the two antiparallel β sheets, one between subunits A and C, the other between subunits B and D (overlap of the two sheets could be unambiguously excluded from a qualitative interpretation of the NOE data as well as considerations of symmetry), and intersubunit NOEs that could not be partitioned into particular intersubunit interactions and were therefore treated as r_{ij}^{-6} sum averages (where r is distance) to allow the computer to partition any given restraint between all pairwise subunit interactions [M. Nilges, *Proteins Struct. Funct. Genet.* 17, 297 (1993)]. With this pairing of the β strands, the interactions between the A and B subunits are symmetrically equivalent to those between the C and D subunits, the interactions between the A and C subunits are symmetrically equivalent to the interactions between the B and D subunits, and the interactions between the A and D subunits are symmetrically equivalent to those between the B and C subunits. In addition to the initial structure calculations, a physical model was built on the basis of the data and proved to be very helpful in sorting out the tetramer arrangement. Once the tetramer topology was clearly established from the initial structure calculations, an iterative strategy was used to assign all structurally useful intra- and intersubunit NOEs explicitly. The final structure calculations were based on 3252 approximate interproton distance

restraints (2412 intra- and 840 intersubunit, partitioned into 758 for the AC and BD subunits, 72 for the AB and CD subunits, and 10 for the AD and BC subunits). These were supplemented by 160 distance restraints for 68 intra- and 12 intersubunit hydrogen bonds, 268 torsion angle restraints (144 ϕ , 104 χ_1 , and 20 χ_2), 144 $^3J_{\text{HN}\alpha}$ coupling constant restraints, and stereospecific assignments for 104 of the 144 β methylene groups and for the methyl groups of all 16 Leu residues. (The number of restraints and stereospecific assignments applies to the tetramer; as the tetramer is completely symmetric, each observed NOE, for example, gives rise to four interproton distance restraints, one for each subunit.) The coordinates of the 30 final simulated annealing (SA) structures of the tetrameric oligomerization domain of p53, together with the coordinates of the restrained minimized mean structure, (SA)r, and the complete list of experimental NMR restraints and ^1H , ^{15}N , and ^{13}C assignments have been deposited in the Brookhaven Protein Data Bank.

10. The precision of the atomic coordinates is defined as the average root mean square difference between the individual simulated annealing structures and the mean coordinate positions. The atoms that do not exhibit conformational disorder comprise all N, C α , C, O, and C β atoms of residues 324 to 356 of the four subunits, the complete side chains of Y327, F328, T329, L330, I332, F338, M340, F341, L344, L348, L350, the side chains of D324, E326, E331, R333, R335, R337, E339, E343, E346, E349, and D352 up to C γ , and the side chains of R24 up to C δ and K351 up to C ϵ (20).
11. C. Chothia *et al.*, *J. Mol. Biol.* 145, 215 (1981).
12. D. Eisenberg and A. D. McLachlan, *Nature* 319, 199 (1986); L. Cliche *et al.*, *Proc. Natl. Acad. Sci. U.S.A.*

87, 3240 (1990).

13. At pH 2.5, the dispersion of the ^1H chemical shifts is typical of a random coil peptide.
14. T. D. Halazonetis and A. N. Kandil, *EMBO J.* 12, 5057 (1993); J. A. Pietenpol *et al.*, *Proc. Natl. Acad. Sci. U.S.A.* 91, 1998 (1994).
15. S. E. Kern *et al.*, *Science* 252, 1708 (1991); W. D. Funk *et al.*, *Mol. Cell. Biol.* 12, 2866 (1992).
16. T. R. Hupp *et al.*, *Cell* 71, 875 (1992).
17. F.-S. Liu *et al.*, *Obstet. Gynecol.* 83, 118 (1994); D. D'Amico *et al.*, *Oncogene* 7, 339 (1992); N. Nishida *et al.*, *Cancer Res.* 53, 368 (1993); H. Miyamoto *et al.*, *Oncology Res.* 5, 245 (1993).
18. G. M. Clore *et al.*, *J. Biomol. NMR* 1, 13 (1991).
19. G. M. Clore *et al.*, *Biochemistry* 29, 1689 (1990); P. J. Lodi *et al.*, *Science* 263, 1762 (1994).
20. Abbreviations for the amino acid residues are: A, Ala; C, Cys; D, Asp; E, Glu; F, Phe; G, Gly; H, His; I, Ile; K, Lys; L, Leu; M, Met; N, Asn; P, Pro; Q, Gln; R, Arg; S, Ser; T, Thr; V, Val; W, Trp; and Y, Tyr.
21. W. DeLano and A. T. Brünger, *AVS-XPLOR User's Manual* (Yale University, New Haven, CT, 1993).
22. M. Carson, *J. Mol. Graphics* 5, 103 (1987).
23. E. De Castro and S. Edelstein, *VISP 1.0 User's Guide* (University of Geneva, Geneva, 1992).
24. B. R. Brooks *et al.*, *J. Comput. Chem.* 4, 187 (1983).
25. Supported by the AIDS Directed Anti-Viral Program of the Office of the Director of NIH (G.M.C., A.M.G., and E.A.). We thank J. Huth for generously providing suitably prepared pET12A vector DNA and M. Greenblatt and C. Harris for useful discussions.

10 May 1994; accepted 13 June 1994

Potential Role of Human Cytomegalovirus and p53 Interaction in Coronary Restenosis

Edith Speir,* Rama Modali, Eng-Shang Huang, Martin B. Leon, Fayaz Shawl, Toren Finkel, Stephen E. Epstein

A subset of patients who have undergone coronary angioplasty develop restenosis, a vessel renarrowing characterized by excessive proliferation of smooth muscle cells (SMCs). Of 60 human restenosis lesions examined, 23 (38 percent) were found to have accumulated high amounts of the tumor suppressor protein p53, and this correlated with the presence of human cytomegalovirus (HCMV) in the lesions. SMCs grown from the lesions expressed HCMV protein IE84 and high amounts of p53. HCMV infection of cultured SMCs enhanced p53 accumulation, which correlated temporally with IE84 expression. IE84 also bound to p53 and abolished its ability to transcriptionally activate a reporter gene. Thus, HCMV, and IE84-mediated inhibition of p53 function, may contribute to the development of restenosis.

Coronary angioplasty causes vessel wall injury and induces a SMC proliferative response similar to the healing response of other tissues to injury. This response is so

excessive in 25 to 50% of patients that it leads to coronary restenosis. On the basis of a proposal that atherosclerosis (also characterized by SMC proliferation) might be a form of benign neoplasia (1), we hypothesized that formation of the neointimal lesion during restenosis may be driven by alterations that confer to cells a selective growth advantage; upon activation, as by injury, such cells would undergo excessive proliferation.

We investigated two molecular mechanisms that might contribute to the abnormal SMC proliferation: (i) aberrant expression of p53, a tumor suppressor protein that inhibits cell cycle progression and

that is functionally inactivated in many human cancers (2); and (ii) activation of latent HCMV, a herpesvirus that has been associated with the development of atherosclerosis (3). Conceivably, an HCMV protein or proteins could impair p53's growth suppressor function, as is the case for proteins encoded by several DNA tumor viruses (4, 5).

We studied 60 patients (age 36 to 89 years; mean 59) who had undergone primary balloon angioplasty for severe symptoms secondary to coronary artery disease. Each had a satisfactory angiographic result at the time of angioplasty but later developed recurrent angina and were subsequently found to have stenosis at the site of angioplasty. Coronary atherectomy was performed 1 to 6 months after angioplasty, and the specimens obtained from such patients are referred to here as restenosis lesions. Atherectomy tissue was also obtained from an additional 20 patients who were undergoing atherectomy for angina but who had not previously undergone angioplasty. These specimens are referred to as primary lesions. The restenosis lesions were firm, cylindrical fragments 1 to 5 mm long and 0.2 to 0.4 mm in diameter. They were cellular and nearly all cells were identifiable as SMCs by immunostaining with an antibody to muscle actin (6). In contrast, primary lesions were hypocellular and often contained thrombus.

In normal cells, wild-type p53 has a short half-life (5 to 20 min) (7) and hence

E. Speir, T. Finkel, S. E. Epstein, Cardiology Branch, National Institutes of Health, Bethesda, MD 20892, USA.

R. Modali, BioServe Biotechnologies Limited, Laurel, MD 20707, USA.

E.-S. Huang, Lineberger Comprehensive Cancer Center, University of North Carolina, Chapel Hill, NC 27599, USA.

M. B. Leon, Washington Cardiology Center, Division of Cardiology, Washington Hospital Center, Washington, DC 20010-2975, USA.

F. Shawl, Department of Cardiology, Washington Adventist Hospital, Takoma Park, MD 20912, USA.

*To whom correspondence should be addressed.

is immunohistochemically undetectable (8). In cancers in which p53 loses its inhibitory function, (usually because of a mutation in the p53 gene), the protein often displays enhanced stability and is detectable by immunostaining (8).

We examined restenosis lesions from 60 patients and found that 23 (38%) were p53-immunopositive [defined as such when $\geq 10\%$ of the SMCs stained with p53-specific antibodies (Fig. 1)]. Of these, 83% contained $\geq 25\%$ immunopositive cells and 60% contained $\geq 50\%$ immunopositive cells. In contrast, none of the 20 primary lesions were p53-immunopositive. It is unlikely that p53-immunopositivity is a consequence of rapid proliferation of SMCs or is a normal feature of the vessel wall as no p53 immunopositivity was found in (i) cultured primary rat and human aortic SMCs that were stimulated by serum (9); (ii) tissue derived from a rat internal carotid artery obtained 2 to 75 days after balloon-induced injury and treated identically to the patient atherectomy specimens (9); (iii) frozen sections of "normal" human coronary arteries from two 18-year-old trauma victims, each having concentric accumulation of SMCs in the neointima (Fig. 1G); and (iv) frozen sections from normal internal mammary arteries obtained from 11 patients undergoing coronary bypass surgery (9).

To determine whether the accumulation

of p53 in the restenosis lesions was due to mutations in the p53 gene, we amplified by polymerase chain reaction (PCR) the genomic DNA of 10 p53-immunopositive lesions (in which $>35\%$ of the SMCs showed immunostaining) with primers complementary to the introns surrounding exons 2 to 11 of the p53 gene (10). Sequencing of the PCR products demonstrated that the lesions contained only wild-type p53 (11).

In certain tumors that are immunopositive for wild-type p53, the protein has been shown to be inactivated and stabilized by interaction with cellular or virally encoded transforming proteins (5, 12). We investigated whether the herpesvirus HCMV was present in the atherectomy specimens because previous studies had demonstrated an association between HCMV infection and atherosclerosis or SMC proliferation (3). In addition, other herpesviruses had been shown to induce SMC proliferation and atherosclerotic-like lesions in the coronary arteries and the aorta of chickens (Marek's disease virus) (13) and in aortic allografts placed into rats (rat CMV) (14).

We used PCR analysis to search for HCMV sequences in 24 human restenosis lesions, 13 of which were p53-immunopositive ($>35\%$ of the SMCs showed immunostaining) and 11 of which were p53-immunonegative. There was a significant concordance between p53 immunoreactiv-

ity and the presence of the HCMV genome; amplified viral-specific PCR products were found in 11 of 13 (85%) of the p53-immunopositive lesions, but in only 3 of 11 (27%) of the p53-immunonegative lesions ($P < 0.01$). Conversely, almost 80% of the HCMV-positive lesions (11 of 14) were p53-immunopositive. None of the 11 primary lesions analyzed by PCR contained HCMV sequences (15).

To determine whether HCMV sequences in the restenosis lesions could express HCMV gene products, we immunostained SMCs cultured from atherectomy specimens with antibodies specific for two major immediate-early proteins, IE72 and IE84 (the 72- and 84-kD products of the HCMV IE1 and IE2 genes, respectively). These viral proteins are expressed in many cell types whether or not viral replication ensues and are believed to be involved in activating the cellular DNA replication machinery (16). We focused mainly on IE84 because it transactivates a variety of heterologous promoters (17). We found that SMCs from four of nine specimens were immunopositive for IE84 and for p53 at passages 1 and 2, whereas the remaining five cultures were immunonegative for both.

The concordance between p53 accumulation and IE84 expression raised the possibility that IE84 might functionally interact with p53. To test this idea, we determined whether HCMV infection of SMCs affects p53 accumulation. Normal human coronary SMCs were infected with HCMV and assayed immunohistochemically for p53 and IE84. The SMCs, initially immunonegative for p53 and

Fig. 1. A restenosis lesion (24) immunopositive for p53 from a patient who had undergone coronary angioplasty 4 months earlier. Tissue was stained with antibody 1801 to p53 (A, E, and G), antibody HHHF35 to muscle actin (B), antibody CM-1 to p53 (C), Movat pentachrome (extracellular matrix is blue, collagen is yellow, and muscle is red) (D), and MOPC 21 (nonimmune mouse myeloma protein) (F). Shown in (G) is a normal human coronary artery. Magnification: (A, B, and F) $\times 28$, (C, D, and E) $\times 173$, and (G) $\times 8$.

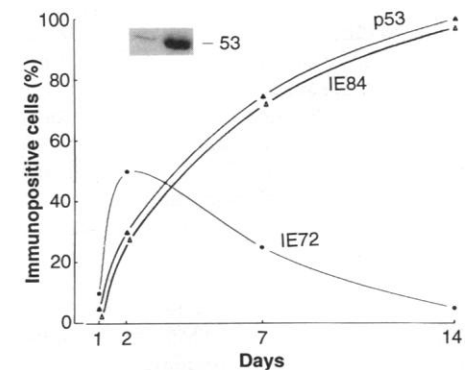
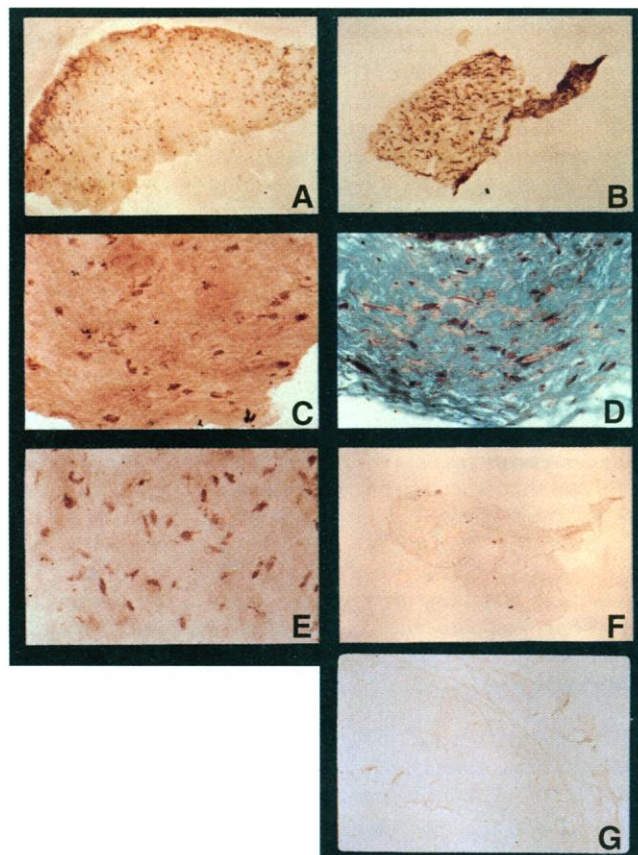
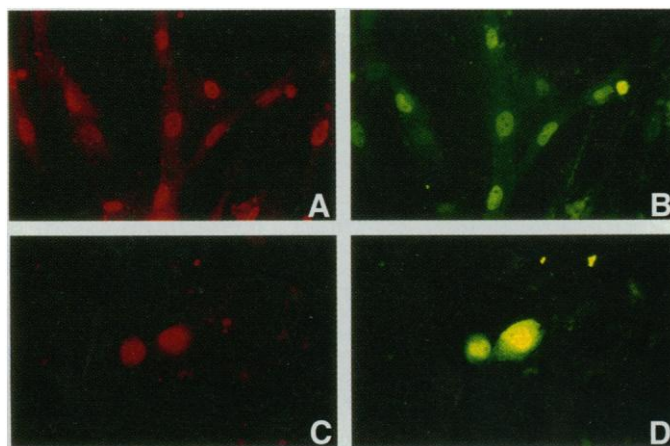


Fig. 2. Time-dependent expression of IE72, IE84, and p53 in human coronary SMCs infected with HCMV at a multiplicity of infection of 10 (25). After fixation and staining with immunoperoxidase, the cells were dehydrated in graded alcohols, then in xylenes, and mounted on cover slips. The ratio of infected cells (brown nuclei) to uninfected cells was determined by counting 100 cells per well, in duplicate wells. Shown in the insert is an immunoblot of SMC lysates probed with an antibody to p53 (1801). The left lane contains uninfected cells and the right lane contains cells harvested 72 hours after HCMV infection.

Fig. 3. Double immunofluorescence staining (26) of HCMV-infected human coronary SMCs for IE84 (red) and p53 (green). (A and B) A colony of SMCs with normal morphology 24 hours after infection. Most of the cells that were immunopositive for IE84 were also immunopositive for p53. (C and D) Two SMCs with virus-mediated cytomegaly 72 hours after infection are intensely stained for both IE84 and p53. A phase-contrast micrograph of the same field as (C) and (D) showed that the cells around the immunopositive cells did not exhibit cytomegaly and were not stained for either protein (9). As controls, infected cells were treated with nonimmune primary antibodies, and uninfected cells were treated with immune primary antibodies (9). Magnification $\times 24$.



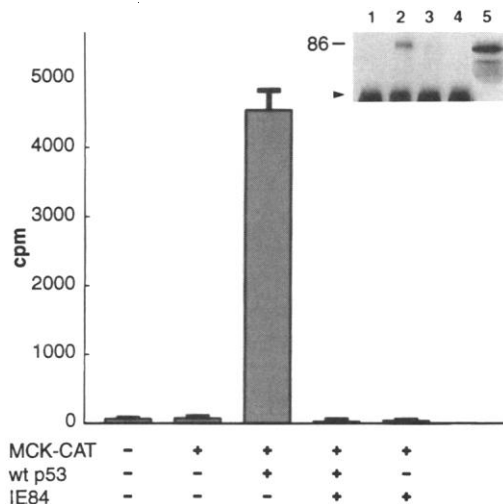
IE84, became immunopositive for both proteins within 2 days after infection, and there was a striking similarity in the kinetics of accumulation of the two proteins (Fig. 2). Immunoblotting with a p53-specific antibody confirmed that HCMV infection leads to p53 accumulation (Fig. 2; insert). IE72 was expressed earlier and more transiently than IE84 (18). Double immunofluorescence staining revealed that IE84 and p53 accumulated in the same cells (Fig. 3).

We next determined whether IE84 alters p53 function, in particular, its ability to stimulate transcription. Human coronary SMCs were cotransfected with plasmids encoding wild-type p53, the HCMV IE84 gene, and a chloramphenicol acetyl transferase (CAT) re-

porter construct (19). Although p53 alone efficiently transactivated the reporter gene, this activity was abolished when p53 was co-expressed with IE84 (Fig. 4).

To investigate whether IE84 physically interacts with p53, we expressed the two proteins individually or together in insect cells using a baculovirus system (20). Cell lysates were first immunoprecipitated with an antibody to p53 (Fig. 4, insert; lanes 1 to 4) and then probed with an IE84-specific antibody by immunoblotting (21). IE84 was indeed detectable in the p53 immunoprecipitate (Fig. 4, lane 2), suggesting that the viral protein mediates its effects on p53, at least in part, through a protein-protein interaction. A small amount of IE84 was consistently seen on

Fig. 4. Detection of a functional interaction between p53 and HCMV in primary human coronary SMCs. Plasmid p50-2 contains two copies of the 50-bp p53-responsive element of the murine muscle creatine kinase (MCK) promoter positioned upstream of the CAT reporter gene; plasmid p11-4 plasmid contains a murine wild-type p53 cDNA under the control of the SV40 promoter (19); plasmid pRc/RSVIE84 contains cDNA encoding HCMV IE84 under the control of the RSV promoter (27). Separate transfection studies demonstrated that IE84 did not inhibit the transcriptional activity of the SV40 promoter. Shown in the insert is an immunoblot analysis of p53-IE84 interaction. Lysates were prepared from insect cells that were uninfected (lane 1), doubly infected with baculoviruses encoding p53 and IE84 (lane 2), infected with a baculovirus encoding p53 only (lane 3), or infected with a baculovirus encoding IE84 only (lane 4). Lysates were precipitated with antibody 1801 to p53, analyzed by SDS-polyacrylamide gel electrophoresis, transferred to nitrocellulose, and then probed with antibody 12E2 to IE84. The presence of the IgG heavy chain at 50 to 55 kD (arrowhead) precluded the reciprocal co-immunoprecipitation. Total cell lysate from HCMV-infected human embryonic lung fibroblasts (HEL) cells was loaded in lane 5 as a positive control for IE84. cpm, counts per minute. Molecular size of 86 kD is indicated.



the immunoblots in the absence of p53 (Fig. 4, lane 3), indicating that some IE84 may bind nonspecifically to the protein A-Sepharose beads. Similar nonspecific binding was seen when an irrelevant first antibody was used. We estimated that less than 10% of the p53 and IE84 in the cells were in a stable complex under the conditions used.

Given that HCMV infection can cause proliferation of a variety of cells (16) including SMCs (22), that herpesviruses can cause atherosclerotic-like lesions in animals (13), and that latent herpesviruses can be reactivated (23), we propose the following model for restenosis. Angioplasty-induced injury to the vessel wall may reactivate latent HCMV, which in turn may cause multiple cellular changes and predispose SMCs to proliferate. Although there are many mechanisms by which HCMV could potentiate the development of restenosis, our data point to a role for viral protein IE84 in blocking p53's inhibition of cell cycle progression. It is of interest that restenosis shares many pathophysiologic features with atherogenesis, and that atherosclerotic vessels often contain HCMV. Conceivably, HCMV-mediated inhibition of p53 may also be important in the development of atherosclerosis and may in part explain the monoclonality observed in some atherosclerotic lesions (1).

REFERENCES AND NOTES

- E. P. Benditt and J. M. Benditt, *Proc. Natl. Acad. Sci. U.S.A.* **70**, 1753 (1973).
- B. Vogelstein, *Nature* **348**, 681 (1990).
- J. L. Melnick, E. Adams, M. E. DeBakey, in *Frontiers of Virology*, Y. Becker, G. Darai, E. S. Huang, Eds. (Springer-Verlag, New York, 1993), vol. 2, chap. 4.
- B. A. Werness, A. J. Levine, P. M. Howley, *Science* **248**, 76 (1990).
- D. I. Linzer and A. J. Levine, *Cell* **17**, 43 (1979); D. P. Lane and L. V. Crawford, *Nature* **278**, 261 (1979); P. Samow, Y. S. Ho, J. Williams, A. J. Levine, *Cell* **28**, 387 (1982); L. Szekeley, G. Selivanova, K. Magnusson, G. Klein, K. Wirnon, *Proc. Natl. Acad. Sci. U.S.A.* **90**, 5455 (1993); Q. Zhang, D. Gutsch, S. Kenney, *Mol. Cell. Biol.* **14**, 1929 (1994).
- T. Tsukada, D. Tippens, D. Gordon, R. Ross, A. M. Gown, *Am. J. Pathol.* **126**, 51 (1987). We used monoclonal antibody HHF35 at 1:12,000 dilution.
- M. Oren *et al.*, *Mol. Cell. Biol.* **1**, 101 (1981); N. C. Reich *et al.*, *ibid.* **3**, 2143 (1983); A. Rogel *et al.*, *ibid.* **5**, 2851 (1985).
- W. P. Bennett *et al.*, *Oncogene* **6**, 101 (1991).
- E. Speir *et al.*, unpublished results.
- T. A. Lehman, W. P. Bennett, R. A. Metcalf, J. A. Welsh, J. Ecker, *Cancer Res.* **51**, 4090 (1991).
- The PCR direct sequencing method allows detection of mutant p53 alleles in a background of 90% wild-type p53 sequences. (C. Harris, personal communication). Because most lesions contained 50 to 75% immunopositive cells, a mutated allele would compose 25 to 35% of the total p53 DNA population and therefore would be detectable in our assays.
- J. D. Oliner *et al.*, *Nature* **358**, 80 (1992).
- C. G. Fabricant *et al.*, *J. Exp. Med.* **148**, 335 (1978).
- K. B. Lemstrom *et al.*, *J. Clin. Invest.* **92**, 549 (1993).
- DNA was extracted from one 50- μ m frozen section and extracts (5 μ l) were tested for HCMV sequences by PCR. A 511-base pair (bp) product of the transforming region or a 240-bp product of the IE2 region

of HCMV was amplified (95°C for 25 s, 42°C for 15 s, and 72°C for 60 s; 40 cycles) with the following primers: AAGCTTGTGTTTTCGAACAT and TTTAT-TGTTCTGCTCCTCTC [J. A. Nelson, B. Fleckenstein, G. Jahn, D. A. Galloway, J. K. McDougall, *J. Virol.* **49**, 109 (1984)]; or for the IE2 region, TCCTCCTGCAGTTCGGCTC and TTTCATGATA-TTGCGCACCT [E. S. Huang and T. F. Kowalik, in (3), vol. 2, p. 247]. Each 100- μ l reaction mixture contained 50 mM tris-HCl (pH 9.0), 3 mM MgCl₂, 40 pmol of each primer, 200 μ M of each deoxynucleotide triphosphate, 5 U of Ampliqaq (Cetus), and 50 ng of genomic DNA.

16. T. Albrecht, I. Boldogh, M. P. Fons, T. Valyin Nagy, in (3), vol. 2, chap. 19.

17. C. Hagemeier *et al.*, *J. Virol.* **66**, 4452 (1992).

18. R. M. Stenberg *et al.*, *ibid.* **63**, 2699 (1989).

19. G. P. Zambetti *et al.*, *Genes Dev.* **6**, 1143 (1992).

20. The coding region of p53 was cloned into pAcJUV51 (Pharmingen) baculovirus transfer vector under control of the p10 promoter. The coding region of HCMV IE84 was cloned into pVL 1392 (Pharmingen) vector under control of the polyhedrin promoter. *Spo-doptera frugiperda* (Sf9) cells were grown at 27°C in Grace's media (Gibco) containing 10% heat-inactivated fetal bovine serum (FBS). The Invitrogen XPRESS SYSTEM was used for transfection and generation of high-titer virus stock. The Sf9 cells (2 \times 10⁷ per 100-mm dish) were infected with recombinant viruses, harvested 72 hours later, and lysed in 0.4 ml of lysis buffer [50 mM tris-HCl (pH 8.0), 150 mM NaCl, 0.5% NP-40, leupeptin (25 mg/ml), and 0.35 mM phenylmethylsulfonyl fluoride]. Lysates were clarified by centrifugation and used for immunoprecipitations.

21. Lysates (~400 μ g) were incubated at 4°C overnight with 1 μ g of antibody 1801, and the antigen-antibody complexes then collected with protein A-Sepharose CL-4B (Pharmacia). Pellets were washed in lysis buffer, resuspended in 40 μ l of loading buffer, and subjected to electrophoresis on an SDS-polyacrylamide gel. The separated proteins were transferred to a nitrocellulose filter, which was then incubated at 4°C overnight in TBST [10 mM tris (pH 8.0), 150 mM NaCl, and 0.05% Tween 20] plus 5% nonfat dry milk. The filter was incubated for 2 hours with an IE84-specific antibody (12E2; 1 μ g/ml), washed in TBST, and then re-incubated with a sheep antibody to mouse immunoglobulin G (IgG) coupled to horseradish peroxidase (1:25,000 dilution). After further washes, the filter was developed with an Ecl detection kit (Amersham).

22. J. J. Tumilowicz *et al.*, *J. Virol.* **56**, 839 (1985).

23. I. Gurevich, *Heart Lung* **21**, 85 (1992).

24. Fresh atherectomy specimens were obtained in the catheterization laboratory from 60 patients with restenosis. Tissue fragments (1 to 5 mg) were embedded in freezing compound, frozen in isopentane-dry ice, and cut into 10 to 20 sections of 6 μ m each; two sections of 50- μ m thickness were cut for DNA isolation and PCR [P. H. Gumerlock, U. R. Poonawallee, F. J. Meyers, W. D. White, *Cancer Res.* **51**, 1632 (1991)]. Sections were placed on polylysine-coated slides and stored at -80°C until processed for staining. The sections were thawed at 22°C, fixed in -20°C methanol, air-dried for 30 min, rehydrated in phosphate-buffered saline (PBS), and processed as in E. Speir *et al.* [*Circ. Res.* **71**, 251 (1992)]. The first and second sections were stained with hematoxylin-eosin and Movat pentachrome, respectively. Subsequent sections were stained with the following antibodies to p53: monoclonal Pab 1801, -421, and -240 at 2 μ g/ml (Oncogene Science, Uniondale, NY) and polyclonal CM1 at 1:1000 [C. A. Midgley *et al.*, *J. Cell Sci.* **101**, 183 (1992)]. For nonimmune controls we used mouse myeloma protein Mopc21 (Cappel, Durham, NC) and normal rabbit serum (Sigma).

25. SMCs (passage 5, grown from explants of a 1-cm segment of human coronary artery obtained at autopsy of an 18-year-old trauma victim, from National Disease Research Interchange, Philadelphia, PA) were seeded at 20,000 cells per well in eight-chamber glass slides (Nunc) and grown in

Medium 199, 20% FBS, 1% antibiotic-antimycotic for 72 hours. After removal of the medium, the cells were infected with 50 μ l of viral supernatant for 2 hours. The virus suspension was then removed and replaced with 0.4 ml of growth medium. Four wells each of infected or uninfected controls for each time point were analyzed by immunocytochemistry. Cells were fixed, incubated with monoclonal antibodies 6E1 (to IE72) or 12E2 (to IE84) (Vancouver Biotech.) or with p53-specific antibodies 1801 or 421 overnight at 4°C, then reacted with biotinylated goat antibody to mouse IgG and ABC complex (Vector Labs) and with diaminobenzidine [E. Speir *et al.*, in (24)]. Whereas IE72 expression was maximal at 48 hours after infection and then declined, IE84 expression was low at 48 hours but was apparent in 70% of the infected cells at 7 days and in 100% of the cells at 14 days after infection.

26. For indirect immunofluorescence, human coronary SMCs at passage 5 were seeded at 30,000 per square centimeter in eight-well glass chamber slides in Medium 199 and 10% FBS and grown for 48 hours. After three washes with warm PBS, cells were fixed in 1% paraformaldehyde for 2 min, then in 50% acetone-methanol at -10°C for 7 min. Cells were then air-dried, washed in PBS, and blocked with 1% goat serum (Vector Labs) for 20 min. Antibody 12E2 (50 μ l), diluted 1:200 in 0.1% crystalline bovine serum albumin (BSA), was added to the wells for 1 hour at 22°C. Cells were washed in warm PBS and the lissamine-rhodamine conjugated goat secondary antibody (Jackson ImmunoResearch, West Grove, PA; diluted in 1% rabbit serum in PBS at 1:50) was added for 30 min at 37°C. Cells were again

washed with warm PBS and polyclonal antibody CM1 (Signet, Dedham, MA; diluted 1:200 in 0.1% BSA) was added to the wells for 1 hour at 22°C. Cells were washed in PBS, fluorescein isothiocyanate-conjugated secondary antibody [diluted in 1% rabbit IgG in PBS (Vector Labs) at 1:50] was added for 30 min, and the cells were washed again. Finally, cells were mounted in 0.1% *p*-phenylenediamine dissolved in PBS (pH 8), and adjusted with carbonate buffer (pH 9.0).

27. The complete coding region of IE2 was PCR-amplified from complementary DNA (cDNA) and cloned into the pRC/RSV expression vector with Hind III and Xba I linkers. Human coronary SMCs were grown in Medium 199 and 10% FBS for 48 hours, then synchronized with 5 mM thymidine for 24 hours [E. Speir and S. E. Epstein, *Circulation* **86**, 538 (1992)] and transiently transfected by lipofection (Dotap, Boehringer) with 2 μ g of each plasmid and 1 μ g of the reporter plasmid p50-2. The results are the average CAT activity of duplicate samples. Three separate transfections were performed. Cell extracts were prepared by three freeze-thaw cycles and then measured for CAT activity with [¹⁴C]chloramphenicol and butyryl coenzyme A [T. Finkel, J. Duc, E. R. Fearon, C. V. Dang, G. F. Tomaselli, *J. Biol. Chem.* **268**, 5 (1993)].

28. We thank J. Griner, B. Choi, and M. Seddon for technical support; R. Guzman for the balloon-injured rat carotid tissue; W. John Martin for the CMV-positive and CMV-negative DNA; R. Dreyfuss for the photomicrography; A. Gown for HHF35; C. Midgley for CM-1; and A. Levine for plasmids p50-2 and p11-4.

7 December 1993; accepted 13 May 1994

Mitotic Regulation of Microtubule Cross-Linking Activity of CENP-E Kinetochores Protein

Hong Liao, Gang Li, Tim J. Yen*

CENP-E is a kinesin-like protein that is transiently bound to kinetochores during early mitosis, becomes redistributed to the spindle midzone at anaphase, and is degraded after cytokinesis. At anaphase, CENP-E may cross-link the interdigitating microtubules in the spindle midzone through a motor-like binding site at the amino terminus and a 99-amino acid carboxyl-terminal domain that bound microtubules in a distinct manner. Phosphorylation of the carboxyl terminus by the mitotic kinase maturation promoting factor (MPF) inhibited microtubule-binding activity before anaphase. Thus, MPF suppresses the microtubule cross-linking activity of CENP-E until anaphase, when its activity is lost.

Chromosome segregation is a highly complex process that relies on the interactions between microtubules of the spindle and a chromosomal domain called the kinetochore. This microtubule-kinetochore connection is essential for the alignment of chromosomes to the metaphase plate as well as for their separation toward opposite ends of a dividing cell. CENP-E is a 312-kD protein that belongs to the kinesin superfamily of microtubule-based motors (1). The subcellular distribution of CENP-E changes markedly during the cell cycle (1, 2). CENP-E is initially detected as a diffuse cytoplasmic protein in cells that are in the

late stages of the cell cycle (G₂ and prophase). It is associated with the kinetochores at prometaphase, but this interaction persists only to metaphase. At anaphase, CENP-E dissociates from the kinetochores and is redistributed to a set of fibers in the spindle midzone. CENP-E becomes concentrated into the midbody at telophase and is degraded after cytokinesis. The specific localization of CENP-E at the kinetochores and the spindle midzone suggests that it may be one of the motors underlying chromosome movement as well as spindle pole elongation during anaphase B (3, 4).

The localization of CENP-E to the spindle midzone during anaphase may reflect cross-linking of the overlapping microtubules within this region because CENP-E appears to

Fox Chase Cancer Center, 7701 Burholme Avenue, Philadelphia, PA 19111, USA.

*To whom correspondence should be addressed.